Construction and Building Materials 147 (2017) 388–397

Contents lists available at ScienceDirect

Construction and Building Materials

journal homepage: www.elsevier.com/locate/conbuildmat

Behaviour of unconfined and FRP-confined rubberised concrete in axial compression

Samar Raffoul *, Reyes Garcia, David Escolano-Margarit, Maurizio Guadagnini, Iman Hajirasouliha, Kypros Pilakoutas

Dept. of Civil and Structural Engineering, The University of Sheffield, Sir Frederick Mappin Building, Mappin Street, Sheffield S1 3JD, UK

HIGHLIGHTS

- Stress-strain behaviour of concrete with high percentage of rubber is examined experimentally.
- External FRP confinement is used to enhance mechanical properties of rubberised concrete (RuC).
- RuC early micro-cracking and lateral expansion is exploited to improve confinement effectiveness.
- Confinement improves RuC compressive strength by 10 times and yields ultimate axial strains of 5%.
- CRuC is suitable for structural applications with high strength and deformability requirements.

ARTICLE INFO

Article history:
Received 12 October 2016
Received in revised form 21 April 2017
Accepted 23 April 2017
Available online 29 April 2017

Keywords:
Tyre rubber
Rubberised concrete
FRP confinement
Highly-deformable concrete

ABSTRACT

This article investigates the use of externally bonded Fibre Reinforced Polymer (FRP) jackets to develop a novel high-strength, highly-deformable FRP Confined Rubberised Concrete (CRuC). Sixty rubberised concrete (RuC) cylinders were tested in axial compression. The cylinders were produced using recycled tyre rubber to replace i) 0–100% fine or coarse aggregate volume or ii) a replacement of 40% or 60% of the total aggregate volume. Six cylinders of the latter mix were then confined with either two or three layers of Aramid FRP sheets. The results indicate that the use of high rubber contents in concrete lead to premature microcracking and lateral expansion, the latter of which can be used to activate the FRP confinement earlier and achieve higher confinement effectiveness. The CRuC cylinders reached compressive strengths of up to 75 MPa and unprecedented ultimate axial strains up to 5%, i.e. about fourteen times larger than those of normal concrete (0.35%). Such novel high-strength, highly-deformable CRuC is of great value to engineers and can be used for structural applications where large deformability is required.

1. Introduction

Worldwide tyre production is forecast to exceed 2.9 billion units per year by the end of 2017 [1] and it is estimated that for every tyre placed in the market, another tyre reaches its service life and becomes waste [2]. Over 300 million tyres reach their service life every year in the EU alone. Whilst stringent EU directives control waste tyre disposal [3], waste tyres are still landfilled and can cause major public health risks and environmental issues. This has increased the efforts towards generating innovative applications for scrap tyres and their main components (vulcanised rubber, steel wire and textile fibres) in the construction industry [4–6].

Vulcanised rubber used in tyre manufacturing has good strength and flexibility and an ability to maintain its volume under compressive stress. Over the last few years, extensive research has investigated the use of recycled tyre rubber as mineral aggregate replacement in concrete. The results from these studies indicate that, compared to normal concrete, rubberised concrete (RuC) has higher deformation capacity [7,8] and vibration damping [9–11]. Conversely, RuC has lower compressive strength, tensile strength and stiffness [12–16]. The compressive strength of RuC with high rubber contents (replacement volumes >50–60%) can be up to 90% lower than that of normal concrete [12,13,17,18]. Such low strength can be mainly attributed to the a) low stiffness and high Poisson's ratio of rubber, resulting in stress concentrations within the mix, b) hydrophobic nature of rubber, which causes weak rubber-cement matrix bonding, c) increased mix non-homogeneity, d) increased porosity and air content, and e) lower "mass stiffness" of RuC [14–16]. The inclusion of rubber in

* Corresponding author.
E-mail address: sraffoul1@sheffield.ac.uk (S. Raffoul).

http://dx.doi.org/10.1016/j.conbuildmat.2017.04.175
0950-0618/

concrete also affects its mix fresh properties, leading to high segregation and bleeding, high air content, as well as low slump and workability [17,19–21]. Whilst considerable amount of literature has been published on RuC, there is a general lack of consensus on the influence of rubber on the physical and mechanical properties of fresh and hardened concrete. Due to the insufficient understanding of the influence of rubber on the mechanical properties of concrete, to date RuC is mainly used in low-strength, non-structural applications such as concrete pedestrian blocks, traffic barriers or lightweight fills [18,21–23].

More recently, limited research has examined the use of Fibre Reinforced Polymer (FRP) sheets to confine RuC specimens (containing low rubber contents) in an attempt to develop adequate axial strength and exploit the potential deformation capacity that RuC can offer [24–28]. Li et al. [25] tested confined rubberised concrete (CRuC) cylinders cast in prefabricated Glass FRP (GFRP) pipes. Whilst the GFRP CRuC specimens were up to 5.25 times stronger than the equivalent unconfined RuC specimens, relatively low compressive strengths of 16.3–22.9 MPa were achieved. Moreover, maximum axial strain values of only about 2.5% could be developed, which are similar to what can be achieved with GFRP confined cylinders made of conventional concrete [29]. Youssf et al. [24] tested CRuC cylinders cast in preformed Carbon FRP (CFRP) tubes. The compressive strength of these cylinders ranged from 61.7 MPa (for one CFRP layer) to 112.5 MPa (for three CFRP layers), thus being suitable for structural applications. However, the deformability potential from using rubber particles was not fully exploited, since the stress-strain behaviour of the CFRP CRuC cylinders [24] was similar to that of CFRP-confined cylinders with conventional concrete [29]. More recently, Duarte et al. [27] tested short RuC columns confined with cold formed steel tubes. Whilst the column ductility was increased by up to 50%, the capacity of the specimens was limited by the premature local buckling of the steel tubes. It should be noted that the studies discussed above only made use of low rubber contents, replacing about 30% of the fine aggregates [25], or 10% [24] and 15% [27] of the total aggregates, and provide evidence that the use of small volumes of rubber aggregate replacement has a minor effect on concrete deformability. The use of higher rubber contents has been previously associated with several material and technological issues and, only recently, work by the authors [30] has successfully addressed some of these challenges and enabled the development of a modified concrete with high rubber contents (>50%) suitable for the manufacture of highly deformable CRuC (axial strains >5%) elements for structural applications.

This article summarises the methodology implemented for the development of improved rubber modified concrete mixes and investigates experimentally the use of externally bonded FRP confinement to exploit the deformation capacity of RuC and develop high-strength, highly-deformable FRP CRuC elements. The results presented in this article are part of the ongoing EU-funded project Anagennisi, which investigates the innovative reuse of all tyre components in concrete [31]. This work is expected to contribute towards the understanding of the mechanical behaviour of FRP CRuC and towards the development of a highly-deformable concrete for high-value structural applications.

2. Experimental programme

The mechanical performance of RuC (with and without FRP confinement) was investigated experimentally using a total of 66 cylinders (100 × 200 mm) cast from 15 different mixes. The main parameters investigated were the effect of rubber content, rubber type and the number of FRP layers on the stress-strain behaviour of RuC up to peak stress.

2.1. Materials

2.1.1. Concrete and rubber

All mixes were produced using CEM II-52.5 N Portland Limestone Cement, containing around 10–15% Limestone in compliance with BS EN 197-1 [32]. Two types of commercial high-range water reducing admixtures [33,34] were used. The fine aggregates were medium grade river washed sand from Shardlow, Derbyshire (UK) with size: 0–5 mm, specific gravity: 2.65, water absorption: 0.5%, and fineness modulus: 2.64. The coarse aggregates were round river washed gravel from Trent Valley (UK) with sizes: 5–10 and 10–20 mm, specific gravity: 2.65, and water absorption: 1.24%.

To examine the influence of rubber type and content on the stress-strain behaviour of RuC, rubber particles were used to replace either a) fine aggregates (sand) by 0–100% by volume, b) coarse aggregates (gravel) by 0–100% by volume, or c) both fine and coarse aggregates by 40% and 60% by volume. The rubber particles were obtained from mechanical shredding of vehicular tyres and had a rough, jagged surface with traces of contamination from steel and polymer fibres. The rubber particles (shown in Fig. 1) were classified as follows: a) fine rubber particles (size 0–5 mm) used as sand replacement, and b) coarse rubber particles (sizes 5–10 mm and 10–20 mm) used as gravel replacement. Fig. 2 shows the particle size distribution of the rubber aggregates determined according to ASTM C136 [35]. Table 1 summarises the physical properties of rubber and mineral aggregates. The rubber particle density and water absorption, flakiness index and bulk density were obtained following Annex C of BS EN 1097-6 (lightweight aggregates) [36], BS EN 933-3 [37] and BS EN 1097-3 [38], respectively. It should be noted, however, that these tests could not be performed on the fine rubber particles (size 0–5 mm) as these float in water and agglomerate due to surface tension and inter-particular forces.

2.1.1.1. Mix design. Previous research by the authors [30] indicated that the inclusion of large volumes of rubber in concrete could lead to very unstable mixes with high levels of segregation and a lack of cohesion, accompanied with significant compressive strength reductions. To minimise such adverse effects, the authors investigated the various mix parameters that influence RuC and proposed an 'optimised' mix design [30] that results in a concrete with good fresh properties (homogeneity and cohesion) and enhanced compressive strength. For instance, when compared to a non-optimised mix with 100% fine rubber replacing sand, the 'optimised' mix was 2.6 times stronger (average strengths of 3.7 and

Fig. 1. Rubber particles used to replace sand (size: 0–5 mm) and gravel (sizes: 5–10 mm and 10–20 mm).

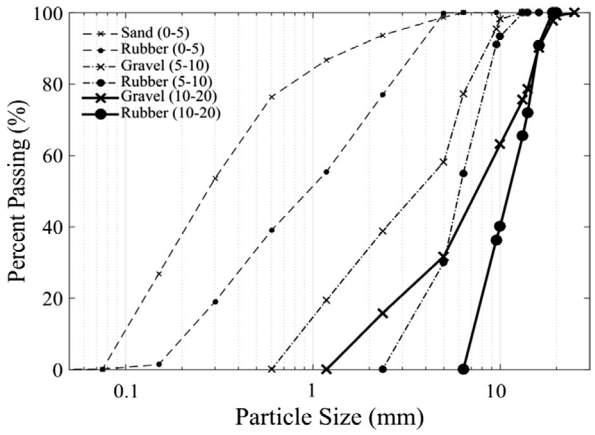

Fig. 2. Sieve analysis of rubber and mineral aggregates.

9.6 MPa, respectively). The 'optimised' mix proportions, used in this study, are presented in Table 2. The mix was designed to be highly flowable with relatively high cement content and water to binder ratio (w/b = 0.35). Rubber contents varied from 0 to 100% of the fine (F) or coarse (C) aggregate volume. A replacement of both fine and coarse mineral aggregates (F&C) was also examined so as to maximise the total volume of rubber in the mix. This comprised: i) a replacement of 40% fine aggregate and 40% coarse aggregate by volume (40F&C, i.e. 40% replacement of the total aggregate volume with rubber), or ii) a replacement of 60% fine aggregate and 60% coarse aggregate by volume (60F&C, i.e. 60% replacement of the total aggregate volume with rubber). Table 3 summarises the rubber and mineral aggregate proportions used for the RuC mixes in this study.

The concrete constituents were mixed as follows: 1) the aggregates (both mineral and rubber) were dry-mixed for 30 s (all mineral aggregates were Saturated Surface Dry (SSD), whereas the rubber particles were mixed dry and as-received), 2) half of the mixing water was added and mixed for another minute, 3) the mix was allowed to rest for three minutes, 4) the binder materials and the remaining mixing water were then added followed by a gradual addition of the admixtures, and 5) the concrete was then mixed for another three minutes. The cylinders were cast in two layers and vibrated on a vibrating table (15–20 s per layer). After casting, the specimens were covered with plastic sheets and kept under standard laboratory conditions for 48hrs. They were then demoulded and stored in a mist room for another 25 days.

2.1.2. FRP confinement

In an effort to develop highly deformable RuC, six cylinders of mix 60F&C were confined with two or three layers of FRP sheets using a wet lay-up technique. Aramid FRP (AFRP) was selected as confining material as it combines good tensile strength and high ultimate elongation. The mean mechanical and physical properties

Table 2
Mix proportions for the optimised mix used in this study.

Material	Quantity
CEM II – 52.5 MPa	340 kg/m^3
Silica Fume (SF)	42.5 kg/m^3
Pulverised Fuel Ash (PFA)	42.5 kg/m^3
Aggregates 0/5 mm	820 kg/m^3
Aggregates 5/10 mm	364 kg/m^3
Aggregates 10/20 mm	637 kg/m^3
Water	150 l/m^3
Plasticiser (P)	2.5 l/m^3
Superplasticiser (SP)	5.1 l/m^3

of the unidirectional AFRP sheets, as provided by the manufacturer, were: tensile strength f_f = 2400 MPa, modulus of elasticity E_f = 116-GPa, ultimate elongation of the fibres ε_{fu} = 2.5%, and thickness of sheet t_f = 0.2 mm. Before applying the AFRP confinement, the surface of the cylinders was brushed and cleaned to improve adherence. To avoid direct contact of the loading device platens with the AFRP confinement and prevent the axial load from being transferred directly to the FRP layers during the tests, the total height of the sheets was 180 mm, i.e. 10 mm at the cylinders' top and bottom were unconfined. The sheets were overlapped by a length of 100 mm with the AFRP fibres oriented perpendicular to the cylinders' axes. Acetate sheets were then placed on the exposed surface of the AFRP to achieve a smooth resin layer finish, thus enabling the easy subsequent installation of foil-type strain gauges. These acetate sheets were removed after one day of resin curing.

2.2. Test setup and instrumentation

All cylinders were subjected to compressive load using a 3000 kN capacity compressive machine connected to a data logger. To prevent possible concrete failure due to stress concentrations during testing, the top and bottom of all cylinders were confined using high-strength high-ductility post tensioned metal straps [39] of thickness 0.8 mm and width 13 mm (for unconfined RuC specimens) or 25 mm (for FRP CRuC specimens). Fig. 3 shows the final setup during the test. The cylinders were tested monotonically in load control using a loading rate of 0.25 MPa/s up to failure. For cylinders with very high rubber contents (above 60% F or C replacement), a load rate of 0.1 MPa/s was used to capture the stress-strain behaviour at smaller time steps.

The test rig was designed to measure local and global vertical and horizontal deformations. To measure local strains, 10 mm foil-type electrical resistance strain gauges were fixed on each cylinder at the locations shown schematically in Fig. 4. Two vertical strain gauges (V1 and V2), located at the cylinders' mid-height (180° apart) were used to measure axial strains, whilst three horizontal strain gauges (H1 to H3) placed radially at 120° were used to monitor lateral strains. In the FRP CRuC cylinders, gauge H3 was located in the middle of the overlap of the AFRP sheets. Global axial

Table 1
Physical properties of rubber and mineral aggregates (adapted from Raffoul et al. [30]).

Material (size in mm)	Apparent density (t/m^3)	Oven dry density (t/m^3)	SSD[a] density (t/m^3)	Water absorption (%)	Specific gravity	Bulk density (t/m^3)	Flakiness Index
Rubber (0–5)	0.80[b]	–	–	–	–	0.40–0.46	N/A
Rubber (5–10)	1.10–1.20	1.00–1.10	1.10–1.2	5.30–8.90	1.10	0.45	6.6–8.3
Rubber (10–20)	1.10	1.10	1.10	0.80–1.30	1.10	0.48	10.4–17.5
Sand (0–5)	2.65	2.62	2.63	0.50	2.65	1.78	N/A
Gravel (5–10)	2.69	2.60	2.63	1.24	2.65	1.51	7.1
Gravel (10–20)	2.69	2.60	2.63	1.24	2.65	1.58	9.7

[a] Saturated Surface Dry.
[b] Average from literature (see [30]).

Table 3
Proportions of rubber and mineral aggregate at different levels of replacement.

Replacement Type	ID	Mass of rubber (kg/m^3)		Mass of CA[a] (kg/m^3)	Mass of FA[a] (kg/m^3)
		C	F		
None	Plain	–	–	1001.0	820.0
Fine Rubber (F)	10F	–	24.8	1001.0	738.0
	20F	–	49.5	1001.0	656.0
	40F	–	99.0	1001.0	492.0
	60F	–	148.5	1001.0	328.0
	100F	–	247.6	1001.0	0.0
Coarse Rubber (C)	10C	30.2	–	900.9	820.0
	20C	60.4	–	800.8	820.0
	40C	120.9	–	600.6	820.0
	60C	181.3	–	400.4	820.0
	100C	302.2	–	0.0	820.0
Fine & Coarse Rubber (F&C)	40F&C	120.9	99.0	600.6	492.0
	60F&C	181.3	148.5	400.4	328.0

[a] CA = coarse aggregate, FA = fine aggregate.

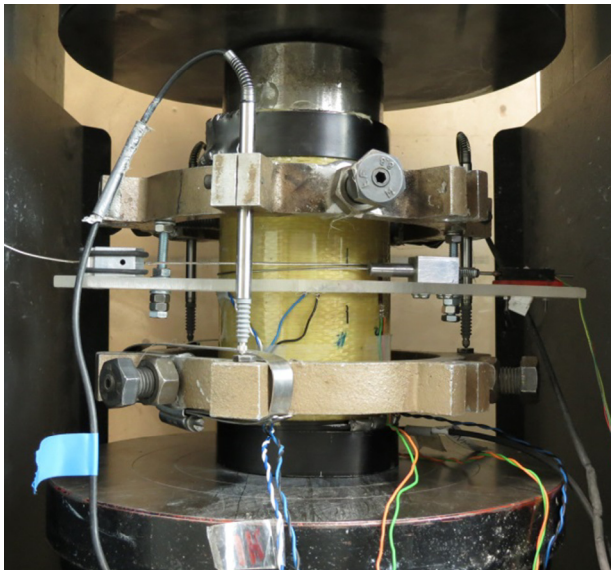

Fig. 3. General view of test setup.

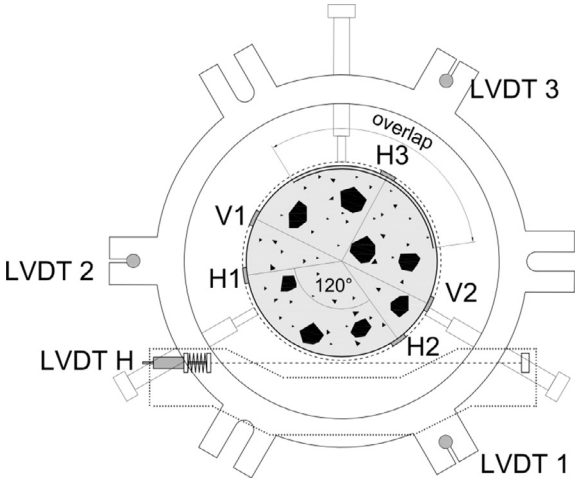

Fig. 4. Typical instrumentation used to test the cylinders.

displacements were monitored using three LVDTs mounted radially at 120° on two steel rings (LVDTs 1–3 in Fig. 4) located at the cylinders' mid-height. The steel rings were fixed to the cylinders using three clamp screws with a centre-to-centre distance of 100 mm. Global horizontal displacements (lateral expansion) were obtained using readings from a LVDT attached to a pre-tensioned circumferential wire around the mid-height of the cylinders (LVDT H).

3. Results and discussion: unconfined RuC

Table 4 summarises the unconfined compressive strength (f_c), initial modulus of elasticity (E_c), absolute values of axial (ε_{cp}) and lateral (ε_{clp}) strains at f_c, as well as the axial strains at the limit of proportionality (LOP), which indicates the onset of microcracking, (ε_{cLOP}). The table also includes the ratio $\varepsilon_{cp}/\varepsilon_{cLOP}$ and the rubber content as a percentage of the total aggregate volume. The compressive strength (f_c) results listed in Table 4 were obtained from at least 4 cylinders per rubber content to account for strength variability, whereas stress-strain results, also discussed in following sections, were obtained for one cylinder per rubber content. The following sections discuss the results of this phase of the testing programme and summarise the most significant observations. It should be noted that a few test data in Table 4 are not reported due to premature failure of the test setup/instrumentation.

3.1. Failure modes

All plain (0% rubber) and RuC cylinders with low rubber contents (10–20% F or C replacement) failed suddenly in an explosive manner. However, the failure of RuC cylinders with more than 40% coarse or fine rubber replacement was more gradual as the cylinders experienced a large amount of fine microcracks and bulging at the mid-height prior to failure (see Fig. 5). This bulging can be attributed to significant lateral dilation produced by the rubber. Overall, the use of metal straps was successful at preventing local failures at the top and bottom of the cylinders.

3.2. Stress-strain behaviour

Fig. 6a-c show the 7-day axial compressive stress against axial and lateral strains obtained from cylinders with F, C and F&C rubber replacement, respectively. In Fig. 6a-c, the axial strain is shown as positive, whereas the lateral strain is shown as negative. It should be noted that the axial strain results in Fig. 6 were obtained

Table 4
Results from unconfined RuC with different rubber contents.

ID	Total aggregate replaced (%)	f_c (MPa)	ε_{cLOP} (με)	ε_{cp} (με)	ε_{clp} (με)	E_c (GPa)	$\varepsilon_{cp}/\varepsilon_{cLOP}$
Plain	0	61.7 ± 4.1	550	2180	885	39.4	3.96
10F	4.5	53.4 ± 2.1	560	1900	890	38.8	3.39
20F	9.0	43.2 ± 4.3	415	1840	1000	35.6	4.43
40F	18.0	32.0 ± 0.9	–[b]	–[b]	1745	–[b]	NA
60F	27.0	20.6 ± 1.0	–[b]	–[b]	1280	–[b]	NA
100F	45.0	9.6 ± 0.7	150	1140	1925	19.9	7.60
10C	5.5	45.9 ± 3.1	390	1830	695	38.7	4.69
20C	11.0	35.5 ± 6.4	310	1590	700	37.0	5.13
40C	22.0	25.3 ± 4.0	290	1670	–[b]	26.9	5.76
60C	33.0	15.8 ± 4.3	230	1430	3040	20.5	6.22
100C	55.0	8.7 ± 1.4	150	1080	1440[b]	14.0	7.20
40F&C	40.0	10.5 ± 0.0[a]	125	1320	3005	18.3	10.56
60F&C	60.0	7.1 ± 1.2	135	1420	3565	11.4	10.52

[a] Only two 40F&C RuC cylinders were tested.
[b] Premature failure of test setup and/or instrumentation.

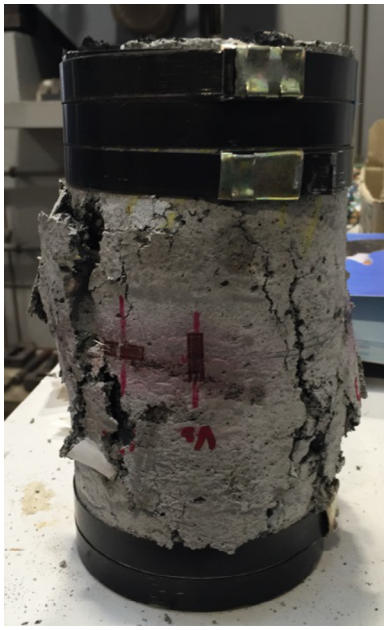

Fig. 5. Typical failure of 60F&C RuC cylinders.

using average global measurements from LVDTs and verified using data from strain gauges (V1 and V2 in Fig. 4). Unfortunately, in the unconfined RuC specimens the circumferential wire often only started recording readings when relatively high lateral strains (above 500με) were reached in the strain gauges. Consequently, Fig. 6 and Table 4 show the average of the three horizontal gauges (H1-H3 in Fig. 4). Note that due to issues in the instrumentation/test setup no axial strain measurements were recorded for 40F and 60F, whereas the lateral strain measurements of 40C were unreliable. Since one of the gauges measuring lateral strains failed at around 1100με, the lateral strain of mix 100C is shown up to that point only.

A linear regression analysis was used to determine the LOP, i.e. the point where the axial stress-strain graph deviates from its initial linear behaviour. In the following sections, the stress and strains at LOP are used to compare cracking and volumetric behaviour of RuC and plain concrete specimens, and to examine the overall effect of rubber on concrete performance.

Fig. 6a indicates that for relatively low fine rubber contents (i.e. 10F and 20F), the axial and lateral strains of RuC are similar to those of plain concrete. For instance, mixes 10F and 20F had 12% and 27% reduction in compressive strength, respectively, whereas their axial strains (ε_{cp} of 1900με and 1840με, respectively) and lateral strains (ε_{clp} of 890με and 1000με, respectively) at peak stress were similar to those of conventional concrete (see also Table 4). Conversely, more significant changes are observed in the RuC stress-strain behaviour at higher fine rubber contents (i.e. 40F, 60F and 100F), especially in terms of lateral strain behaviour. For instance, mix 100F experienced 118% increase in ε_{clp} and 48% reduction in ε_{cp} compared to the plain mix.

A similar trend was observed in mixes with coarse aggregate replacement (see Fig. 6b and Table 4). In this case, all mixes experienced a reduction in ε_{cp} and an increase in ε_{clp} when compared to the plain mix (except for mixes 10C and 20C with lower ε_{clp}). Compared to the plain mix, ε_{cp} of mix 60C was reduced by 35% (1430με), whereas ε_{clp} increased by 245% (3040με). A larger reduction in axial strain was observed for 100C (50% reduction in ε_{cp} over the plain mix); however, ε_{clp} was not recorded due to excessive cracking at the cylinder's mid-height, which led to failure in the horizontal gauges (see Fig. 6b).

The combined replacement of fine and coarse aggregates with rubber (mixes 40F&C and 60F&C, see Fig. 6c and Table 4) changes significantly the constitutive behaviour of RuC when compared to mixes with only fine or coarse aggregate replacement. While mixes 40F&C and 100F had similar levels of total aggregate replacement (40% and 45% of the total aggregates replaced, respectively), ε_{clp} of mix 40F&C was 55% higher. Mix 60F&C exhibits the largest increase in lateral strain capacity (around 300% increase over the plain mix), reaching ε_{clp} of 3565με. The large lateral expansion in some mixes with high levels of C or F&C replacement (as opposed to F replacement) can be attributed to a higher local expansion of rubber particles, particularly if strain gauges happened to be placed near large coarse rubber particles, but also due to the rubber's ability to hold the concrete together and maintain its integrity as lateral strains increase, as proven by previous research [4,11,17,40].

Overall, the results in Fig. 6 show that RuC cylinders with low rubber contents (<18% of the total aggregate volume) behave similarly to plain concrete and therefore have limited lateral expansion. This could explain why previous research on CRuC (all using rubber contents below 15% of the total aggregate volume [24,25,27]) showed that the concrete volumetric behaviour changed only marginally, compared to confined conventional concrete. Conversely, the observed axial and lateral strain behaviour of RuC with high rubber contents (>27% of the total aggregate volume) is heavily influenced by the low stiffness and high Poisson ratio of

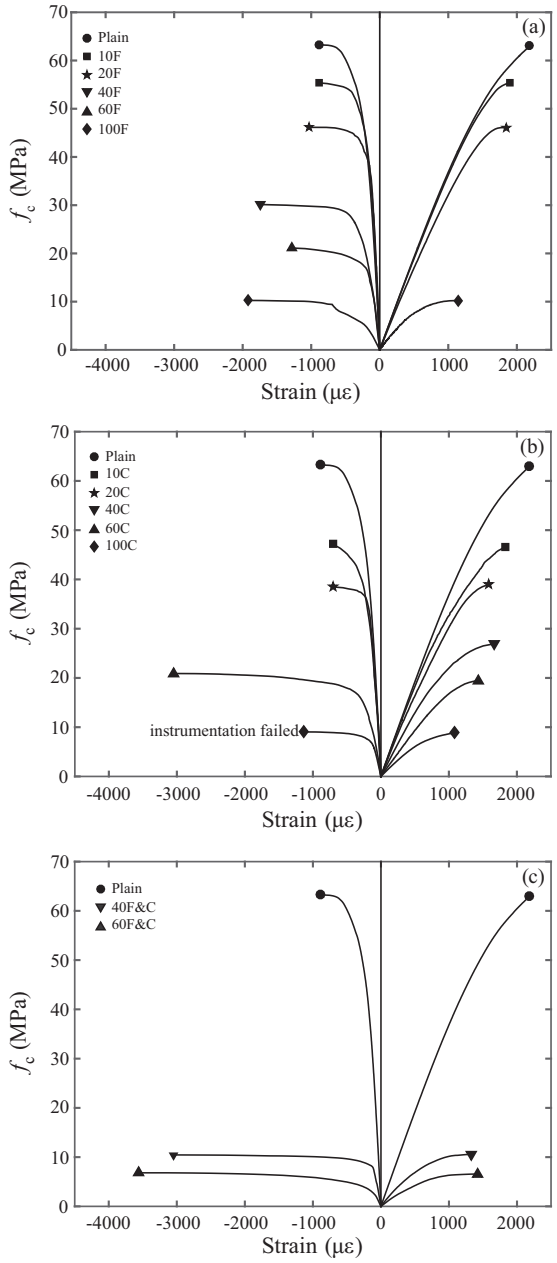

Fig. 6. Uniaxial compressive stress-strain behaviour of unconfined RuC with a) fine rubber replacement (F), b) coarse rubber replacement (C), and c) combined replacement of fine and coarse rubber (F&C).

rubber. When a RuC cylinder is subjected to axial load, rubber tends to expand laterally more than the surrounding concrete. This results in tensile stress concentrations in the concrete around the rubber and in the premature formation of micro-cracks, thus leading to unstable crack propagation and failure of RuC at lower peak axial strain when compared to conventional concrete. Premature micro-cracking and rubber expansion also increases the concrete overall volumetric expansion. This unique feature (and disadvantage) of RuC with high rubber contents can be used to activate the confining pressure of CRuC earlier than in confined conventional concrete.

Previous research by the authors [30] showed that the compressive strength of RuC mixes with similar percentages of total volume of fine or coarse aggregate replacement with rubber is similar. Based on this observation, Fig. 7a–d compare the stress

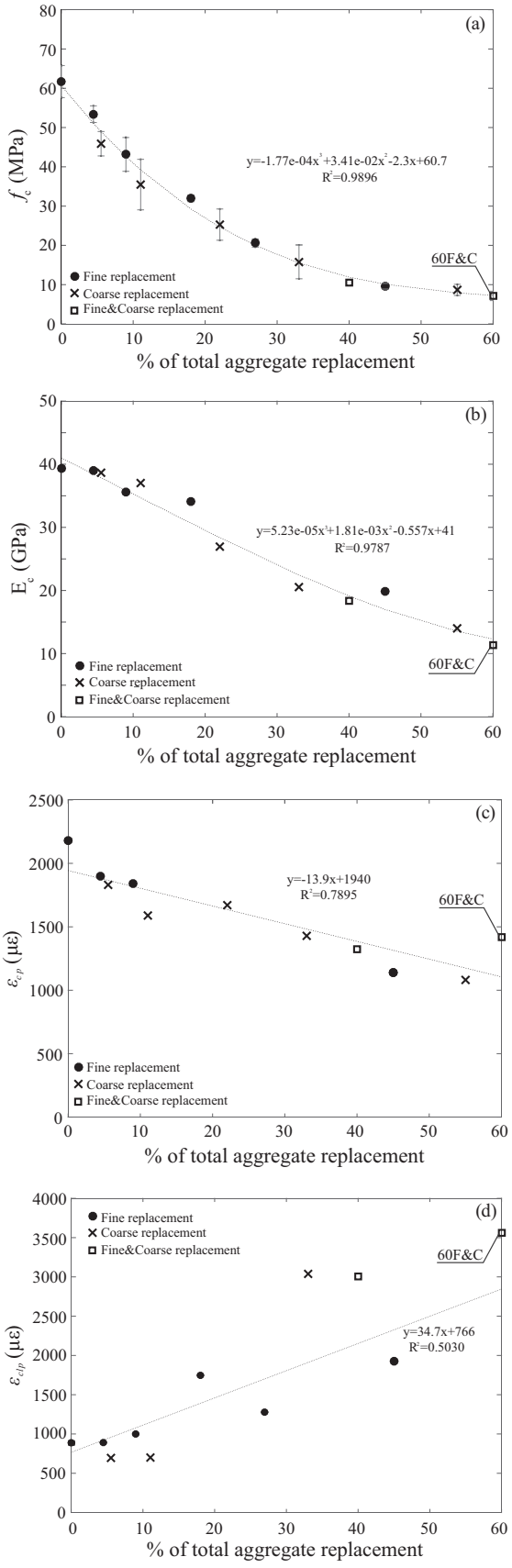

Fig. 7. Variation in a) stress, b) modulus of elasticity, c) peak axial strain, and d) peak lateral strain as function of the percentage of total aggregate volume replaced with rubber.

(f_c), modulus of elasticity (E_c), axial strain (ε_{cp}), and lateral strain (ε_{clp}) at peak stress, respectively, as a function of the total aggregate volume replaced with rubber. As expected, the results in Fig. 7a confirm that regardless of the type of rubber replacement (C, F or F&C), the strength of RuC mixes reduces with increasing rubber content (up to 90% for mix 60F&C with the highest total aggregate replacement). However, the rate at which the compressive strength reduces is faster at lower rubber contents and seems to stabilise at total rubber contents above 40%, where rubber properties appear to dominate the compressive behaviour of RuC.

Fig. 7b shows that E_c also reduces with increasing rubber content. Such reduction in stiffness can be attributed to the lower stiffness of rubber particles (compared to mineral aggregates) and to the higher air content, as confirmed by previous research [40]. However, E_c seems to be minimally affected by the type of rubber replacement (fine or coarse).

The data in Fig. 7c and Table 4 indicate that the axial strain at peak stress (ε_{cp}) reduces with increasing rubber content. For mixes with high rubber contents (e.g. mix 100C), ε_{cp} was only 50% of the corresponding value for plain concrete (1080με vs 2180με, see Table 4). This reduction in ε_{cp} was also accompanied by a reduction in axial strains at LOP (ε_{cLOP}). For instance, ε_{cLOP} reduced from 550με in the plain mix to 150με for mixes 100F and 100C, and to 135με for mix 60F&C, respectively (see Table 4). This indicates that the onset of localised micro-cracking occurs at earlier stages when large volumes of rubber are added to concrete, thus leading to premature lateral expansion. Whilst both ε_{cp} and ε_{cLOP} reduced with increasing rubber contents, ε_{cLOP} reduced at a faster rate as evidenced by a consistently increasing $\varepsilon_{cp}/\varepsilon_{cLOP}$ ratio (see Table 4) with increasing rubber contents (e.g. 4.69 and 10.52 for 10C and 60F&C, respectively).

Although the data obtained from lateral strain gauges may have been affected by high heterogeneity of RuC and local phenomena (such as the high local expansion of large rubber particles), the results in Fig. 7d and Table 4 show clearly that the lateral expansion ε_{clp} of RuC increases with the rubber contents, reaching values of more than 3500με for mix 60F&C (i.e. 4 times the ε_{clp} of the plain mix).

Based on the above discussion, it is evident that the inclusion of high rubber contents in concrete leads to larger lateral expansion and premature unstable crack propagation, which result in low compressive strengths, stiffness and peak axial strains. This effect of rubber content on RuC mechanical performance follows a clear trend (as illustrated in Fig. 7a-d); nevertheless, due to high material heterogeneity and local effects, more work is required to develop accurate predictive models. Whilst the above-mentioned behaviour is highly detrimental for structural unconfined concrete, the premature lateral expansion of RuC can be exploited to activate the (passive) confining pressure provided by FRP, which relies on concrete dilation. In an effort to fully utilise the maximum axial deformability potential of confined RuC, mix 60F&C (with the highest lateral strain capacity) was selected to develop a highly deformable FRP CRuC, as discussed in the following section.

4. Results and discussion: FRP-confined RuC

Table 5 summarises the results of compression tests conducted on six AFRP CRuC cylinders (obtained from the same batch of concrete) in terms of: confined compressive strength (f_{cc}), absolute values of axial strain at LOP (ε_{ccLOP}), ultimate axial strain (ε_{ccu}), lateral strain at LOP (ε_{cclLOP}), ultimate lateral strain (ε_{cclu}), and initial modulus of elasticity (E_c). The confinement effectiveness (f_{cc}/f_c) and ductility ($\varepsilon_{ccu}/\varepsilon_{ccLOP}$) ratios are also included for comparison. In Table 5, the cylinders are identified according to the mix designation (60F&C), the number of confining AFRP layers (2L or 3L) and the specimen number. The following sections discuss the results of this phase of the testing programme and summarise the main experimental observations.

4.1. Failure modes

All specimens failed in an explosive manner dominated by rupture of the AFRP jackets at the cylinders' mid-height (see typical failure in Fig. 8). The horizontal strain gauges recorded strains in the range of 14,660–20,300με, i.e. between 70 and 96% of the theoretical ultimate strains of the AFRP sheet (21,000με). Only minor damage was observed at the top or bottom of the cylinders, which indicates that the metal straps successfully prevented concrete crushing at these regions. Unfortunately, the straps of cylinders 60F&C-2L-1 and 60F&C-3L-3 failed prematurely and therefore these tests had to be halted.

4.2. Stress-strain behaviour

The results in Table 5 indicate that the use of two (2L) or three (3L) AFRP layers enhanced the compressive strength of CRuC by an average of 7.3 and 10.1 times over RuC, respectively. Likewise, axial strains reached an average of 4.2% and 4.8% in CRuC (excluding cylinders with instrumentation failure) with 2L or 3L of AFRP confinement, respectively. Fig. 9a shows the compressive stress vs

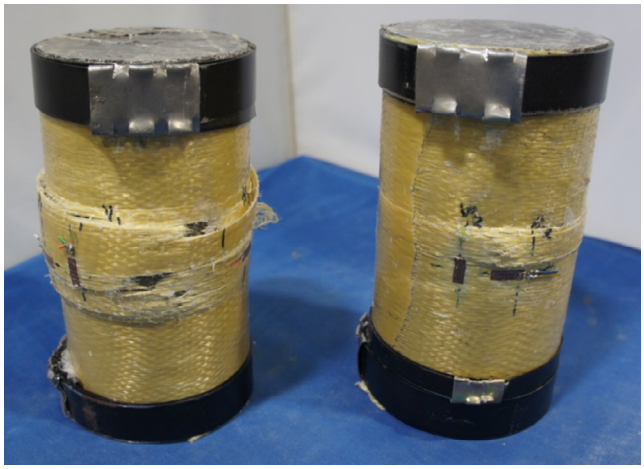

Fig. 8. Typical failure modes of AFRP CRuC cylinders.

Table 5
Main results from AFRP CRuC cylinders.

ID	# of layers	f_{cc} (MPa)	ε_{ccLOP} (με)	ε_{ccu} (με)	ε_{cclLOP} (με)	ε_{cclu} (με)	E_c (GPa)	f_{cc}/f_c	$\varepsilon_{ccu}/\varepsilon_{ccLOP}$
60F&C-2L-1	2	41.0*	1031	27860	640	15555	10.6	6.1	27
60F&C-2L-2	2	49.8	894	37390	523	19490	10.1	7.4	42
60F&C-2L-3	2	56.2	928	46610	381	20300	9.9	8.4	50
60F&C-3L-1	3	74.9	800	49730	302	16210	13.0	11.2	62
60F&C-3L-2	3	73.3	934	46650	293	16270	12.0	10.9	50
60F&C-3L-3	3	62.4*	1200	33450	207	14660	7.3	9.3	28

* Premature failure of test set-up or instrumentation.

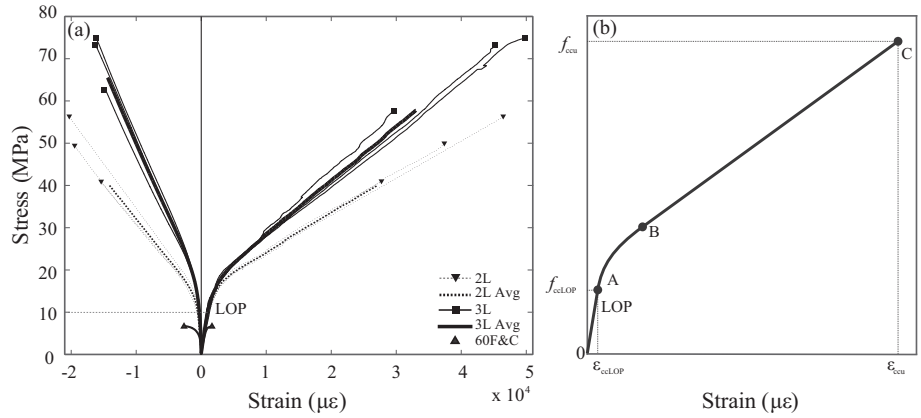

Fig. 9. Axial stress-strain relationships of a) tested CRuC cylinders and b) typical FRP confined concrete.

axial strains (shown as positive) and lateral strains (shown as negative) for the 2L and 3L AFRP CRuC cylinders, as well as the corresponding average results.

The results indicate that the curves of AFRP CRuC have a bilinear shape similar to that of regular FRP confined concrete [41] with two distinctive parts (see Fig. 9b):

1) An initial linear elastic part controlled by the unconfined behaviour of RuC (point 0 to A), where the material reaches the LOP, followed by a transition zone (A to B).
2) A second linear part controlled by the lateral expansion of the AFRP jacket (B to C). The RuC is progressively crushing but it can sustain high axial as well as lateral deformations, the latter enhancing the effectiveness of the AFRP confining jackets.

It should be noted that, in Fig. 9, the axial strains for the initial elastic part (0 to A) were taken as the average readings from the two vertical strain gauges (V1 and V2 in Fig. 4). After point A (i.e. LOP), the measurements from the gauges deviate from those of the LVDTs due to localised bulging of the AFRP sheets in the vertical direction. Therefore, the axial strain measurements after the LOP were taken as the average values of the three vertical LVDTs. The horizontal strains in Fig. 9 were taken as the average from the horizontal strain gauges H1 to H3.

Fig. 9 indicates that the AFRP confinement delays the onset of cracking, which is evident by the increase in the elastic region 0-A in CRuC, when compared to the unconfined RuC with identical rubber content (60F&C in Fig. 9a). This is in agreement with observations reported in previous tests [25]. As shown in Fig. 9a, the stress at LOP was on average 10 MPa, which is 1.5 times larger than the elastic stress for the unconfined 60F&C RuC, with a peak strength of 6.7 MPa (Fig. 9a and Table 4). This can be attributed to the low axial stiffness and large lateral deformation capacity of the RuC mix 60F&C, which engaged the confinement even before the RuC starts cracking. Future research should examine how the amount and type of confinement delay the onset of cracking in different RuC mixes confined with FRP.

4.3. Volumetric strain

To provide further insight into the constitutive behaviour of AFRP CRuC, this section examines the volumetric strain (ε_{vol}) of the tested cylinders. Using the axial and lateral strains recorded during the tests, ε_{vol} can be calculated according to the following equation:

$$\varepsilon_{vol} = \varepsilon_a + 2\varepsilon_l \quad (1)$$

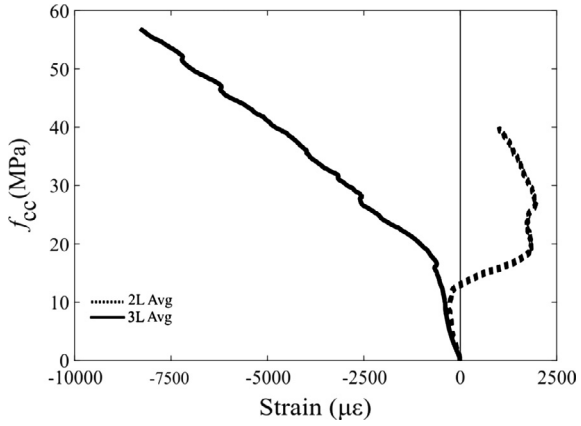

Fig. 10. Axial stress-volumetric strain relationships of CRuC cylinders.

where ε_a is the axial strain (taken as negative for compression), and ε_l is the lateral strain (taken as positive for tension). As such, negative values of ε_{vol} indicate volumetric contraction of concrete, whereas positive values indicate volumetric expansion.

Fig. 10 shows the axial stress vs volumetric strain of AFRP CRuC cylinders. Note that the results are the average of three specimens. It is shown that all AFRP CRuC cylinders contracted at the initial elastic stage,where the curves of CRuC cylinders with 2L or 3L of AFRP were similar. Conversely, after the LOP, specimens 2L experienced expansion, whereas specimens 3L carried on contracting (decrease in overall volume). This behaviour may be attributed to the (incompressible) nature of the rubber particles, which fill up the voids left by crushed/pulverised concrete. Fig. 10 indicates that the volumetric behaviour of AFRP CRuC with 3 layers of AFRP is considerably different to that of RuC cylinders confined with 2 layers of AFRP. Whilst 2 AFRP layers led to RuC expansion after LOP, RuC cylinders confined with 3 AFRP layers did not expand. Nevertheless, further tests are necessary to confirm these results. Current research is also investigating other aspects of FRP CRuC behaviour (e.g. shear and short/long term durability) in order to provide practical design guidelines. These results will be published in future papers.

5. Conclusions

This article investigates the use of externally bonded FRP jackets to develop a new high-strength, highly-deformable FRP CRuC

for structural applications. Sixty RuC and six CRuC standard cylinders were tested in axial compression to evaluate the behaviour of unconfined and confined RuC. Based on the results of this study, the following conclusions can be drawn:

- The stress-strain behaviour of cylinders made with concrete with low rubber contents (less than 18% of the total aggregate volume) is similar to that of conventional concrete. However, even such modest replacement volumes led to large reductions in compressive strength (up to 40% for mix 20C with 11% total aggregate replacement).
- Replacing aggregates with rubber also reduces the axial strain of the resulting concrete at peak stress. This effect was particularly evident for high rubber contents (>27% of the total aggregate volume). As rubber content was increased, the reduction in axial strains was accompanied by a premature onset of localised micro-cracking.
- The difference in compressive strength when comparing fine or coarse aggregate replacement with similar overall aggregate replacement is marginal. The combined replacement of coarse and fine aggregate is the best option to maximise rubber content and deformability potential, while achieving adequate workability.
- Replacing aggregates with rubber increases the lateral deformation capacity of RuC by up to 300% over the plain mix. Confining such RuC with two and three layers of AFRP increased the compressive strength by up to 10.1 times (f_{cc} = 75 MPa) over the control mix. Moreover, average axial ultimate strains of up to 5% were achieved (i.e. 14 times more than conventional concrete). This indicates that CRuC is suitable for structural applications where high deformability is required.
- The lateral confinement modified the volumetric behaviour of CRuC. Specimens with 2 layers of AFRP had volumetric expansion after the LOP, whereas those with 3 layers of AFRP maintained volumetric contraction. This behaviour can be attributed to the incompressible nature of the rubber particles, which can fill the voids in concrete under heavy confinement, leading to overall contraction of the cylinders with 3 AFRP layers.

The results of this study confirm the feasibility of developing highly deformable AFRP CRuC with sufficient strength for structural applications. However, due to the limited experimental data, future research should verify the variability of results and possible size effects. Moreover, the use of more widely available confining materials such as Carbon FRP could be also studied.

Acknowledgements

The research leading to these results has received funding from the European Union Seventh Framework Programme [FP7/2007-2013] under grant agreement n° 603722 and the European Union's Horizon 2020 research and innovation programme under the Marie Sklodowska-Curie grant agreement n° 658248. The authors also thank Richard Morris from Tarmac UK for providing the Portland Limestone Cement (CEM II 52.5 N). The AFRP system was kindly provided by Weber Saint-Gobain, UK.

References

[1] Business T. Global tire sales to grow 4.3% per year. Tire Business, 1/17/2014; 2014.
[2] ETRA. The European Tyre Recycling Association. Available at: http://www.etra-eu.org [Last accessed: 10/06/2014].
[3] Directive (EC) 98/2008 of the European Parliament and of the Council of 19 November 2008 on waste and replacing certain Directives [2008] OJ L312/3.
[4] B.S. Thomas, R.C. Gupta, A comprehensive review on the applications of waste tire rubber in cement concrete, Renew. Sustain. Energy Rev. 54 (2016) 1323–1333.
[5] O. Sengul, Mechanical behavior of concretes containing waste steel fibers recovered from scrap tires, Constr. Build. Mater. 122 (2016) 649–658.
[6] S.-S. Huang, H. Angelakopoulos, K. Pilakoutas, I. Burgess, Reused tyre polymer fibre for fire-spalling mitigation, Appl. Struct. Fire Eng. (2016).
[7] D. Goulias, A.-H. Ali, Evaluation of rubber-filled concrete and correlation between destructive and nondestructive testing results, Cem. Concr. Aggregates 20 (1) (1998) 140–144.
[8] K.S. Son, I. Hajirasouliha, K. Pilakoutas, Strength and deformability of waste tyre rubber-filled reinforced concrete columns, Constr. Build. Mater. 25 (1) (2011) 218–226.
[9] F. Liu, W. Zheng, L. Li, W. Feng, G. Ning, Mechanical and fatigue performance of rubber concrete, Constr. Build. Mater. 47 (2013) 711–719.
[10] J. Xue, M. Shinozuka, Rubberized concrete: a green structural material with enhanced energy-dissipation capability, Constr. Build. Mater. 42 (2013) 196–204.
[11] K.B. Najim, M.R. Hall, Mechanical and dynamic properties of self-compacting crumb rubber modified concrete, Constr. Build. Mater. 27 (1) (2012) 521–530.
[12] M.K. Batayneh, I. Marie, I. Asi, Promoting the use of crumb rubber concrete in developing countries, Waste Manage. 28 (11) (2008) 2171–2176.
[13] Z.K. Khatib, F.M. Bayomy, Rubberized Portland cement concrete, J. Mater. Civ. Eng. 11 (3) (1999) 206–213.
[14] E. Ganjian, M. Khorami, A.A. Maghsoudi, Scrap-tyre-rubber replacement for aggregate and filler in concrete, Constr. Build. Mater. 23 (5) (2009) 1828–1836.
[15] M.C. Bignozzi, F. Sandrolini, Tyre rubber waste recycling in self-compacting concrete, Cem. Concr. Res. 36 (4) (2006) 735–739.
[16] G. Li, M.A. Stubblefield, G. Garrick, J. Eggers, C. Abadie, B. Huang, Development of waste tire modified concrete, Cem. Concr. Res. 34 (12) (2004) 2283–2289.
[17] H.A. Toutanji, The use of rubber tire particles in concrete to replace mineral aggregates, Cement Concr. Compos. 18 (2) (1996) 135–139.
[18] P. Sukontasukkul, C. Chaikaew, Properties of concrete pedestrian block mixed with crumb rubber, Constr. Build. Mater. 20 (7) (2006) 450–457.
[19] A. Turatsinze, J.L. Granju, S. Bonnet, Positive synergy between steel-fibres and rubber aggregates: effect on the resistance of cement-based mortars to shrinkage cracking, Cem. Concr. Res. 36 (9) (2006) 1692–1697.
[20] A.E. Richardson, K.A. Coventry, G. Ward, Freeze/thaw protection of concrete with optimum rubber crumb content, J. Cleaner Prod. 23 (1) (2012) 96–103.
[21] C. Pierce, M. Blackwell, Potential of scrap tire rubber as lightweight aggregate in flowable fill, Waste Manage. 23 (3) (2003) 197–208.
[22] H. Zhu, N. Thong-On, X. Zhang, Adding crumb rubber into exterior wall materials, Waste Manage. Res. 20 (5) (2002) 407–413.
[23] P. Sukontasukkul, Use of crumb rubber to improve thermal and sound properties of pre-cast concrete panel, Constr. Build. Mater. 23 (2) (2009) 1084–1092.
[24] O. Youssf, M.A. ElGawady, J.E. Mills, X. Ma, An experimental investigation of crumb rubber concrete confined by fibre reinforced polymer tubes, Constr. Build. Mater. 53 (2014) 522–532.
[25] G. Li, S.-S. Pang, S.I. Ibekwe, FRP tube encased rubberized concrete cylinders, Mater. Struct. 44 (1) (2011) 233–243.
[26] R. Abendeh, H.S. Ahmad, Y.M. Hunaiti, Experimental studies on the behavior of concrete-filled steel tubes incorporating crumb rubber, J. Constr. Steel Res. 122 (2016) 251–260.
[27] A. Duarte, B. Silva, N. Silvestre, J. de Brito, E. Júlio, J. Castro, Experimental study on short rubberized concrete-filled steel tubes under cyclic loading, Compos. Struct. (2015).
[28] A. Moustafa, M.A. ElGawady, Strain rate effect on properties of rubberized concrete confined with glass fiber-reinforced polymers, J. Compos. Constr. 04016014 (2016).
[29] L. Lam, J. Teng, Ultimate condition of fiber reinforced polymer-confined concrete, J. Compos. Constr. 8 (6) (2004) 539–548.
[30] S. Raffoul, R. Garcia, K. Pilakoutas, M. Guadagnini, N.F. Medina, Optimisation of rubberised concrete with high rubber content: an experimental investigation, Constr. Build. Mater. 124 (2016) 391–404.
[31] Innovative Use of all Tyre Components in Concrete, Anagennisi Project. 2014. Available at: http://www.anagennisi.org/.
[32] BSI 197-1:2011. Cement. Part 1: Composition, specifications and conformity criteria for common cements. 2011, BS EN 197 Part 1. London UK.
[33] Sika Limited. Sika Viscoflow 2000. Product Data Sheet. Edition-15/10/2014; Identification no: 02 13 01 01 100 0 001325. Available at https://goo.gl/kMfHcU [Last accessed 10/12/2015].
[34] Sika Limited. Sika Viscoflow 1000. Product Data Sheet. Edition-21/05/2015; Identification no: 02 13 01 01 100 0 000853. Available at https://goo.gl/mMDfay [Last accessed 10/12/2015].
[35] ASTM Standard C136, Standard Test Method for Sieve Analysis of Fine and Coarse Aggregates, ASTM International, West Conshohocken, PA, 2006, http://dx.doi.org/10.1520/C0136-06.
[36] BSI 1097-6: 2013. Tests for mechanical and physical properties of aggregates. Determination of particle density and water absorption. 2013, BS EN 1097 Part 6. London, UK.
[37] BSI 933-3:2012. Tests for geometrical properties of aggregates. Determination of particle shape – Flakiness index. 2012, BS EN 933 Part 3. London, UK.

[38] BSI 1097-3:1998. Tests for mechanical and physical properties of aggregates: Determination of loose bulk density and voids. 1998, BS EN 1097 Part 3. London, UK.
[39] R. Garcia, K. Pilakoutas, I. Hajirasouliha, M. Guadagnini, N. Kyriakides, M.A. Ciupala, Seismic retrofitting of RC buildings using CFRP and post-tensioned metal straps: shake table tests, Bull. Earthquake Eng. (2015) 1–27.
[40] A. Turatsinze, M. Garros, On the modulus of elasticity and strain capacity of self-compacting concrete incorporating rubber aggregates, Resour. Conserv. Recycl. 52 (10) (2008) 1209–1215.
[41] J. Teng, J.-F. Chen, S.T. Smith, L. Lam, FRP: strengthened RC structures, Front. Phys. 1 (2002).